

Research article

Sepsis-induced inflammatory demyelination in medullary visceral zone and cholinergic anti-inflammatory pathway: Insights from a Rat's model study

Gao Chen^{a,1}, Cheng Zhang^{b,1}, Hongbing Li^b, Xian Liu^{c,*}

^a The Intensive Care Unite of Hubei Cancer Hospital, Tongji Medical College, Huazhong University of Science and Technology, Wuhan, Hubei Province, 430079, China

^b Emergency Department of the First People's Hospital of Guiyang of Guizhou Province, 550002, China

^c Geriatrics Department of the First People's Hospital of Guiyang of Guizhou Province, 550002, China

ARTICLE INFO

Keywords:

Sepsis
Cholinergic anti-inflammatory pathway
Inflammatory demyelination
Heart rate variability
Medullary visceral zone

ABSTRACT

Background: Our previous studies have demonstrated that the activated Cholinergic Anti-inflammatory Pathway (CAP) effectively suppresses systemic inflammation and immunity in early sepsis. Some parameters of Heart Rate Variability (HRV) could be used to reflect the regulatory activity of CAP. However, in the early stages of severe sepsis of some patients, the inflammatory storm can still result in multiple organs dysfunction and even death, suggesting they lose CAP's modulation ability. Since CAP is part of the vagus nerve and is directly innervated by the Medullary Visceral Zone (MVZ), we can reasonably concluded that pathological changes induced by MVZ's neuroinflammation should be responsible for CAP's dysfunction in modulating systemic inflammation in early sepsis.

Methods: We conducted two independent septic experiments, the sepsis model rats were prepared by cecum ligation and puncture (CLP) method. In the first experiment, A total of 64 adult male Sprague-Dawley rats were included. Under the condition of sepsis and CAP's pharmacological activation or blockade, we investigated the MVZ's pathological changes, the functional state of key neurons including catecholaminergic and cholinergic neurons, key genes' expression such as Oligodendrocyte Transcription Factor 2 (Olig-2) mRNA, glial fibrillary acidic protein (GFAP) mRNA, and matrix metalloprotein (MMP) -9 mRNA, and CAP's activities reflected by HRV. The second experiment involved in 56 rats, through central anti-inflammation by feeding with 10 mg/ml minocycline sucrose solution as the only water source, or right vagus transection excepting for central anti-inflammation as a mean of the CAP's functional cancel, we confirmed that the neuroinflammation in MVZ affected systemic inflammation through CAP in sepsis.

Results: In the first experiment, cholinergic and catecholaminergic neurons showed significant apoptosis with reduced expressions of TH, but the expression of CHAT remained relatively unaffected in MVZ in sepsis. HRV parameters representing the tone of the vagus nerve, such as SDNN, RMSSD, HF, SD1, and SD2, did not show significant differences among the three Septic Groups, although they all decreased significantly compared to the Control Group. The expressions of GFAP mRNA and MMP-9 mRNA were up-regulated, while the expression of Olig-2 mRNA was

* Corresponding author.

E-mail addresses: 407349098@qq.com (G. Chen), 1907915805@qq.com (C. Zhang), mrbright789@sina.com (H. Li), 2637117535@qq.com (X. Liu).

¹ Gao Chen and Cheng Zhang have contributed equally to this work and share first authorship.

down-regulated in the Septic Groups. Intervention of CAP had a significant effect on cholinergic and catecholaminergic neurons' apoptosis, as well as the expressions of TH/CHAT and these key genes, but had little effect on HRV in sepsis. In the second experiment, the levels of TNF- α , IL-6, in serum and MVZ were significantly increased in sepsis. Central anti-inflammatory treatment reversed these changes. However, right vagotomy abolished the central anti-inflammatory effect. *Conclusions:* Our study uncovered that MVZ's neuroinflammation may play a crucial role in the uncontrolled systemic inflammation through inflammatory demyelination in MVZ, which disrupts CAP's modulation on the systemic inflammation in early sepsis.

1. Introduction

The Global Sepsis Campaign 2021 acknowledges sepsis as a global health threat, as it continues to pose significant risks to mortality and disability in both acute and chronic stages [1], and imposes a substantial burden on healthcare and economy [2]. The early stage of sepsis often triggers Systemic Inflammatory Response Syndrome (SIRS), leading to early mortality in critically ill patients.

It has been established that the vagus nerve plays an important role in the inflammatory reflex and regulates the strength of inflammation and immunity through the Cholinergic Anti-Inflammatory Pathway (CAP) [3]. This pathway involves the Medullary Visceral Zone (MVZ) in the brainstem as the reflex center, the vagus nerve as the afferent and efferent pathway, and $\alpha 7$ -nicotinic acetylcholine receptors ($\alpha 7$ nAChRs) on the cytomembrane of immune cells as effectors [4]. Together, they collaboratively and negatively regulate systemic inflammation and immunity.

CAP functions by releasing acetylcholine, which acts on $\alpha 7$ nAChRs of T lymphocytes, inhibiting their differentiation into Th1 and Th17 cells, while promoting their division into Th2 and Treg cells. Additionally, acetylcholine binding with $\alpha 7$ nAChRs also inhibits the secretion of pro-inflammatory cytokines [5]. Through these activities, CAP negatively modulates the intensity of immune response and inflammation, thereby aiding in pathogen clearance and restoration of immune homeostasis. Transection of the right cervical vagus nerve in septic rats abolishes CAP's function of inhibiting systemic inflammation and has been shown to result in a large number of deaths in sepsis models [6]. CAP promptly, dynamically, and efficiently modulates systemic inflammation and immunity, playing a critical role in suppressing early systemic inflammatory storms in sepsis [7], as well as regulating local inflammation in organs such as the lungs and kidneys [8,9].

Indeed, heart rate variability (HRV) is a non-invasive method that can be used to indirectly assess the function of the autonomic nervous system (ANS) [10], providing quantitative information about the modulation of sympathetic and parasympathetic nerves on the heart and other internal organs. HRV has been shown to be reduced in sepsis, and changes in HRV may precede the onset of hemodynamic instability in septic patients [11], making it a potential tool for early detection and prognostic assessment in sepsis.

In previous studies [12], researchers have identified specific HRV parameters to evaluate the activity of CAP on inflammation and immune regulation. These parameters include frequency domain parameters such as high frequency (HF), time domain parameters such as standard deviation of all NN intervals (SDNN), the root mean square successive difference (RMSSD), and non-linear parameters such as width of a scatterplot of the deviations of successive pairs of RR intervals (SD1) and length of a scatterplot of the deviations of successive pairs of RR intervals (SD2). These HRV parameters have been shown to be negatively correlated with serum levels of cytokines such as TNF- α , IL-1 α , IL-6, IL-10, sCD14, HMGB1, and lymphocyte ratio of TH17 to CD4⁺CD25⁺Treg, which are markers of systemic inflammation and immune balance. By monitoring changes in HRV, healthcare professionals can evaluate how well the autonomous nervous system is modulating systemic inflammation, offering essential insights into the functional activity of CAP in septic patients [11]. HRV analysis can be a useful tool for evaluating CAP's function in sepsis and may have potential implications for monitoring and managing septic patients.

The medullary visceral zone (MVZ), serving as the integration center of CAP [13], may be susceptible to neuroinflammation induced by sepsis, similar to other central nervous system structures [14,15]. Neuroinflammation has the potential to damage MVZ and disrupt its modulation of the autonomic nervous system [16]. Therefore, neuroinflammation may play a crucial role in the early regulatory disorders of inflammation and immunity in sepsis, although the specific mechanism remains unknown. In addition, what will happen in MVZ under the condition of sepsis and CAP's pharmacological activation (such as GTS-21, a specific agonist of $\alpha 7$ nicotinic acetylcholine receptor, $\alpha 7$ nAChR) or blockade (such as Methyllycaconitine, MLA, the antagonist of $\alpha 7$ nAChR)? Investigating the pathological changes in MVZ induced by neuroinflammation and their impact on CAP's regulation is of significant importance in understanding and correcting early inflammation dysregulation in sepsis.

2. Materials and methods

2.1. Animals

A total of 120 adult specific pathogen-free male Sprague-Dawley (SD) rats, were obtained from the Hubei Provincial Experimental Animal Research Center [License number: SCXK (Hubei) 2020-0018]. The rats were 8 weeks old and weighed between 250 and 280 g at the start of the study. They were housed in the Laboratory Animal Center of the First Hospital of Guiyang, maintained at a controlled temperature of 21 ± 0.5 °C, and subjected to a 12-h light-dark cycle (lights on from 07:00 to 19:00). Standard chow and tap water were provided ad libitum. The rats were acclimatized for 7 days prior to the experimental procedures. All experimental protocols (described

in the section below) were conducted in accordance with the Guidance Suggestions for the Care and Use of Laboratory Animals formulated by the Ministry of Science and Technology of the People's Republic of China (2006 Edition). The study was approved by the Ethics Committee of the Guizhou Medical University, Guizhou Province, China (Approval No.: 2100819).

2.2. Animal grouping and treatment

As reported in previous study [12,17], after 7 days of adaptive feeding the formal experiment begins, 3 days after the relevant intervention, the rats' blood and brain tissue were harvested for detection. The first experiment carry out such analysis as short-term HRV, TdT mediated dUTP Nick End Labeling (TUNEL), Immunofluorescence and Quantitative Reverse Transcription-Polymerase Chain Reaction (RT-PCR). The second experiment involves with Western blot (WB) and Enzyme Linked Immunosorbent Assay (ELISA).

In the first experiment, a total of 64 rats were divided into 3 groups according to the random number table, they were separately treated as follows: ① Control Group (8 rats): rats were fed as usually without any treatment; ② Sham Group (8 rats): rats were subjected to open and suture the abdominal cavity under anesthesia with inhalation of isoflurane [18] without cecal ligation and puncture (CLP) operation, afterwards, they were accepted intraperitoneal injection of piperacillin (50 mg/Kg, qd × 3d); ③ Sepsis Group (48 rats): rats were prepared sepsis models with CLP operation, afterwards, they were randomly divided into 3 groups, 16 rats in each group. a: Model Group: intraperitoneal injection of piperacillin (50 mg/Kg, qd × 3d) and saline (1 ml/100 g, qd × 3d). b: GTS-21 Group, beside piperacillin, intraperitoneal injection of GTS-21 (4 mg/kg, qd × 3d) was given to each rat [19]. c: Methyllycaconitine (MLA) Group: beside piperacillin, intraperitoneal injection of MLA (4.8 mg/kg, qd × 3d) was given to each rat [20].

In the second experiment, a total of 54 rats were divided into four groups, they were separately treated as follows: ① Control Group (8 rats) and ② Model Group (16 rats) were treated as the first experiment. ③ Central Anti-inflammatory Group (16 rats): after 4 days of feeding with 10 mg/ml minocycline phosphate (dissolved in 5 % sucrose solution) as the only water source, rats were treated as the CLP model group. ④ CAP Transection Group, After isolation and transection of the right cervical vagus nerve under anesthetization by inhalation of isoflurane, rats went through adaptive feeding for 7 days, the rest of the treatment was the same as the Central Anti-inflammatory Group.

In these two experiments, except for the died rats, all the survival rats were included in the planned studies.

2.3. Short-term HRV analysis

HRV, which can reflect the overall health status [21], is known to be influenced by injuries and critical illnesses such as sepsis, which can disrupt the functioning of the autonomic nervous system (ANS) and trigger an inflammatory response [22,23]. Reduced vagal innervation has been associated with increased inflammatory response [24]. Stimulation of the vagus nerve (VN) has been shown to suppress blood TNF levels [25]. Non-linear analysis of HRV can provide insights into the complex interactions involving the regulation of the autonomic and central nervous systems. In fact, some HRV parameters have been found to be superior to quick sepsis-related organ failure assessment (qSOFA) score, Modified Early Warning Score (MEWS), and National Early Warning Score (NEWS) in predicting 30-day in-hospital mortality for adults with sepsis [26–28]. These studies highlight that HRV can reflect the regulatory function of VN on systemic inflammation in sepsis. Therefore, we conducted a short-term analysis of HRV in this study.

The short-term HRV (5 min) analysis can stably reflect the general health state [29] and was used to measure the tone of VN of rats in the first experiment. Two hours after intraperitoneal injection, short-term HRV analysis was conducted once a day for three consecutive days using the Noninvasive ECG System (ECGenie™, Mouse Specifics, Inc. in USA) to record ECG signals of rats under unrestrained awake conditions. Two electrodes were fixed on the dorsal surface of the xiphoid process and in the anterior mediastinum after rats were anesthetized with isoflurane inhalation. After approximately 2 h, rats were recovered and HRV recording began. This method allows for wireless collection of 5-min ECG samples, minimizing voltage instability during activities and improving the signal-to-noise ratio [30]. Corrections for isolated ectopic beats were made using cubic spline interpolation starting from the RR intervals unaffected by non-sinus cardiac beats. The corrections did not exceed 1 % of the total beats, as all experimental rats were healthy before the experiment. The parameters were set as follows: sampling rate at 1K/s and low-pass filter at 1 kHz. Frequency domain, time domain, and nonlinear analysis of HRV were performed, including main indicators such as SDNN, RMSSD, total power (TP), very low frequency (VLF), low frequency (LF, 0.2–0.75 Hz), and high frequency (HF, 0.75–2.5 Hz). Lorenz scatter plots were drawn and SD1 and SD2 were calculated using the software. Except for spectral analysis performed via nonparametric analysis, other indexes of HRV adopted parametric analysis.

2.4. TdT mediated dUTP nick end labeling (TUNEL)

After 3 days, rats were euthanized under anesthesia with inhalation of isoflurane [17] to collect the medulla oblongata for reverse transcription-polymerase chain reaction (RT-PCR), TdT mediated dUTP nick end labeling (TUNEL), and Fluorescent immunolabeling analysis. Though these results have been reported in our previous study [12], it is necessary to remind it again.

For TUNEL and Immunofluorescence analysis, paraffin sections of the medulla oblongata were prepared first. After blood collection, rats were perfused transcardially with phosphate-buffered saline (PBS, 0.01 M, 150 mL at pH 7.4) followed by a paraformaldehyde (PFA, 350 mL) solution. Subsequently, the medulla oblongata was harvested and conventionally embedded with paraffin to prepare sections (30 μm). For TUNEL analysis, the sections were dewaxed and immersed in Proteinase K solution. Then, the terminal deoxynucleotidyl transferase (TdT) buffer was added for incubation, followed by 4',6-Diamidino-2-phenylindole (DAPI) (Beyotime Biotechnology, lot number: C1002) and fluorescence quencher (southernbiotech, lot number: 0100–01) to stain the nuclei

and apoptotic cells. Finally, the sections were observed under a fluorescent microscope (Olympus BX53 biological microscope). Image J software (National Institutes of Health, V1.8.0.112) was used to calculate the apoptosis index. Ten images from each group were randomly selected, and the Apoptosis Index (the average ratio of the number of apoptotic cells to the total number of cells in each image) [31] was calculated for each group.

2.5. Immunofluorescence

As it has been reported in our previous study [12], for immunofluorescence analysis, the dehydrated sections were blocked with 10 % normal goat serum for 1 h, followed by incubation for 24 h with a cocktail of primary antibodies for caspase3 (produced by Wuhan Sanyan Bio. Co., China, Lot: 66470-2-IG, dilution: 1:50), tyrosine hydroxylase (TH, produced by Wuhan Boster Co., China, Lot: BM4568, dilution: 1:50), or choline acetyltransferase (CHAT, produced by Wuhan Bioss Co., China, Lot: bs-2423R, dilution: 1:50). After 4 h, sections were incubated with fluorescent-labeled secondary antibodies (FITC labeled goat anti-rabbit IgG, produced by Wuhan Boster Co., China, Lot: BA1105, dilution: 1:100, Cy3 labeled goat anti-mice IgG, produced by Wuhan Boster Co., China, Lot: BA1031, dilution: 1:100). Finally, the sections were mounted on gelatin-coated slides and covered with mounting medium with DAPI to stain the nuclei of all cells present in the slice [32]. Images from the different experimental groups were captured with an Olympus BX53 Biological Microscope. Nine MVZ images with 400-fold enlargement from three rats in each group were analyzed using Image Pro Plus 6.0 (IPP6.0, Mediacybernetics) software [33], and the average optical densities were acquired.

2.6. Quantitative RT-PCR

Fresh tissue samples weighing 0.1 g from the Medulla Oblongata were taken from each group and homogenized in 1 mL of Trizol reagent (Aidlab, Lot:252250AX) using a bead mill (Retsch Tissue Lyzer II, Qiagen, Valencia CA, USA). RNA was extracted and reverse transcribed into cDNA. DNA starting primers were designed, synthesized, and supplied by Qingke Co. Ltd. The sequences are shown in Table 1. Rat β -actin was selected as the inner reference to calculate the expression levels of oligodendrocyte transcription factor 2 (Olig-2) mRNA, glial fibrillary acidic protein (GFAP) mRNA, and matrix metalloprotein (MMP)-9 mRNA. Add the cDNA and the specific primers into Real-time fluorescence quantitative PCR equipment (produced by Eastwin, type: EDC-810) to reaction. Dissolution curves were plotted and final data were analyzed as $2^{-\Delta\Delta C_t}$. The gel imaging system's grayscale scanning software was used to analyze the electrophoresis target zone and acquire the intensity ratios of the target gene compared to the reference gene.

2.7. Western blot assay

In the second experiment, all the survival rats were anesthetized by inhalation of isoflurane, their chests were opened to expose the hearts. Blood samples (8 ml) were collected from the right ventricle and remained for 1h at room temperature, then they were centrifuged at 3000r for 10min to obtain serum for ELISA detection. After blood collection, the rats were perfused with normal saline until the internal organs turned pale, then the medulla oblongata of the rats were got and frozen for WB analysis.

A small amount of medulla oblong tissue was placed in 2 ml EP tubes, and 200 μ l of tissue lysate was added to each tube to lyse cells. Then the total protein was extracted by centrifugation, and protein concentration was determined by BCA method. Equal amount of protein was loaded, denatured and electrophorized on the polyacrylamide gel and then were transferred to polyvinylidene difluoride membranes, followed by blocking with 8 % skim milk at room temperature for 1 h and washing. The membranes were cut into strips and put into the corresponding primary antibodies solution, including: rabbit polyclonal antibody Tumor Necrosis Factor Alpha (TNF- α) (21KD), manufacturer: Biyuntian, batch number: AF8208, dilution ratio: 1:1000; Rabbit polyclonal antibody Interleukin 6(IL-6) (24KD), manufacturer: Affinity, batch number:DF6087, dilution ratio: 1:1000. The solution was incubated overnight at 4 °C on a shaker. The next day, the strips were washed and put into HRP labeled sheep anti-rabbit secondary antibody (manufacturer: Wuhan Boster, batch number: BA10541, dilution ratio: 10,000). The PVDF membrane was immersed in the secondary antibody solution and incubated at room temperature for 2 h on a shaker. Finally, ECL luminescent solution was used for imaging and exposure on a gel imager, and the film gray value was analyzed by ipp6.0 software to calculate the expression level of proteins.

Table 1
Primer sequence list.

Name	Primer	Sequence	Size
Rat β -actin	Forward	5'-CACGATGGAGGGCCGGACTCATC-3'	240bp
	Reverse	5'-TAAAGACCTCTATGCCAACACAGT-3'	
Rat Olig-2	Forward	5'-TCATCTTCCTCCAGCACCTCCTCGT-3'	311bp
	Reverse	5'-TGACCCCGTAAATCTCGCTCACCA-3'	
Rat GFAP	Forward	5'-ACGAACGAGTCTTGGAGAG-3'	181bp
	Reverse	5'-CGATGTCCAGGGCTAGCTTA-3'	
Rat MMP-9	Forward	5'-GCTGGGCTTAGATCATCTTCAGTG-3'	109bp
	Reverse	5'-CAGATGCTGGATGCCTTTATGTCTG-3'	

2.8. Enzyme linked immunosorbent assay (ELISA) test (kit)

According to the instructions of the ELISA kit, 10ul rat's serum was added into the sample well of the plate, and the corresponding standard well was set up at the same time. The plate was gently shaken and then incubated at 37 °C for 2 h. After washing and drying, 100ul biotin-labeled antibody working solution was added, including Rat TNF- α , batch number: MM-0180R1, manufacturer: elabscience; Rat IL-6, batch number: MM-0190R1, Manufacturer: elabscience. Afterwards, the plates were incubated at 37 °C for 1 h prior to be dried and washed for 3 times. At last, 50 μ L of chromogenic A and B were added to each well, and the optical density (OD) value of each well was measured at 450 nm wavelength by a spectrophotometer reader within 10 min after stopping reaction. The concentrations of various inflammatory molecules were calculated.

2.9. Statistics

All data were presented as mean \pm standard deviation (mean \pm SD) and analyzed as measurement data. Statistical analysis was performed using SPSS 19.0 software package (SPSS Inc, Chicago, IL, USA). Homogeneity of variance was checked first. In case of positive Levene's test, Dunnett test was used for comparisons. For homogeneous data, analysis of variance (ANOVA) was used to compare differences between any two groups, with Bonferroni Test used for post hoc analysis. For non-homogeneous data, Tamhane Test was used. Correlation analysis between HRV, TUNEL, and immunofluorescence results was conducted using Pearson's or Spearman's Correlation analysis (two-tailed tests). $P < 0.05$ was considered statistically significant.

3. Results

3.1. Mortality rate among different groups

In the first experiment, there were respectively 9, 8, 11 rats died in Model Group, GTS-21 Group and MLA Group, the mortality rates were individually 56.3 %, 50 % and 68.8 %. There was no death in the Control Group and the Sham Group. There was a significant difference in mortality among the five groups ($\chi^2 = 14.21$, $P = 0.003$), but there was no significant difference in mortality among the three septic groups ($\chi^2 = 1.21$, $P = 0.107$).

In the second experiment, there were respectively 0, 10, 4, 7 rats died in the Control Group, Sepsis Group, Central Anti-inflammation Group and CAP Transection Group. the mortality rates were individually 0 %, 62.5 %, 25 % and 43.8 %. There was a significant difference in mortality among the four groups ($\chi^2 = 8.47$, $P = 0.004$).

3.2. HRV analysis

One-way ANOVA was used to compare HRV indicators among the Control Group, the Sham Group, and three Septic Groups. SDNN, RMSSD, HF, SD1, and SD2 were significantly reduced in the three Septic Groups compared to the Control Group and the Sham Group ($P < 0.05$). There were no differences in SDNN, RMSSD, HF, SD1, and SD2 among the three Septic Groups. There were no statistically significant differences in HR, TP, VLF, LF, LF/HF, and SD1/SD2 among the five groups. Refer to [Table 2](#) for details.

Results of this study showed that HRV indices, including SDNN, RMSSD, HF, SD1, and SD2, were significantly lower in the Model Group, GTS-21 Group, and MLA Group compared to the Control Group. There were no significant differences among groups in terms of HR, TP, VLF, LF, LF/HF, and SD1/SD2 ($p < 0.05$).

▲ $P < 0.05$ vs Control Group.

The representative diagrams of HRV ([Fig. 1](#)) revealed that, in comparison to the Control Group and Sham Group, the trend of R–R intervals in the Sepsis Group (comprising of Model Group, GTS-21 Group, and MLA Group) exhibited less fluctuation. There were

Table 2
Analysis of HRV among different groups.

	Control Group	Sham Group	Model Group	GTS-21 Group	MLA Group
HR (bits/min)	253.44 \pm 51.33	223.22 \pm 22.10	287.92 \pm 28.05	284.00 \pm 23.07	274.33 \pm 20.80
SDNN (ms)	3.96 \pm 0.89	4.08 \pm 0.90	1.59 \pm 0.83▲	1.93V \pm 0.74▲	1.89 \pm 0.72▲
RMSSD (ms)	4.25 \pm 1.75	4.34 \pm 1.26	1.69 \pm 1.00▲	2.20 \pm 0.96▲	2.32 \pm 1.03▲
TP (ms2)	1213.27 \pm 1022.20	2101.61 \pm 345.48	1213.48 \pm 818.07	1401.31 \pm 678.42	1572.39 \pm 747.65
VLF (ms2)	957.12 \pm 978.45	1820.08 \pm 368.32	992.03 \pm 808.40	1200.65 \pm 660.70	1370.90 \pm 677.89
LF (ms2)	213.65 \pm 109.33	232.95 \pm 83.31	190.67 \pm 25.46	170.85 \pm 30.96	167.81 \pm 74.43
HF (ms2)	42.56 \pm 17.63	48.56 \pm 13.06	30.75 \pm 5.82▲	29.83 \pm 6.44▲	33.67 \pm 11.17▲
LF/HF	5.20 \pm 2.12	4.79 \pm 1.01	6.45 \pm 1.64	5.99 \pm 1.66	4.75 \pm 2.06
SD1 (ms)	3.00 \pm 1.23	3.07 \pm 0.89	1.19 \pm 0.71▲	1.56 \pm 0.68▲	1.64 \pm 0.73▲
SD2 (ms)	4.64 \pm 1.04	4.78 \pm 1.42	1.87 \pm 1.01▲	2.20 \pm 0.92▲	2.08 \pm 0.77▲
SD1/SD2	0.66 \pm 0.27	0.69 \pm 0.27	0.67 \pm 0.27	0.74 \pm 0.24	0.78 \pm 0.22

The table presents the mean \pm standard deviation of HRV indices over a three-day period. SDNN represents the standard deviation of all RR intervals, RMSSD indicates the root mean square successive difference of continuous RR intervals, TP refers to total power, VLF represents very low frequency, LF denotes low frequency (0.2–0.75 Hz), HF indicates high frequency (0.75–2.5 Hz), SD1 represents the mean width of a scatterplot of successive pairs of RR intervals, and SD2 represents the mean length of a scatterplot of successive pairs of RR intervals.

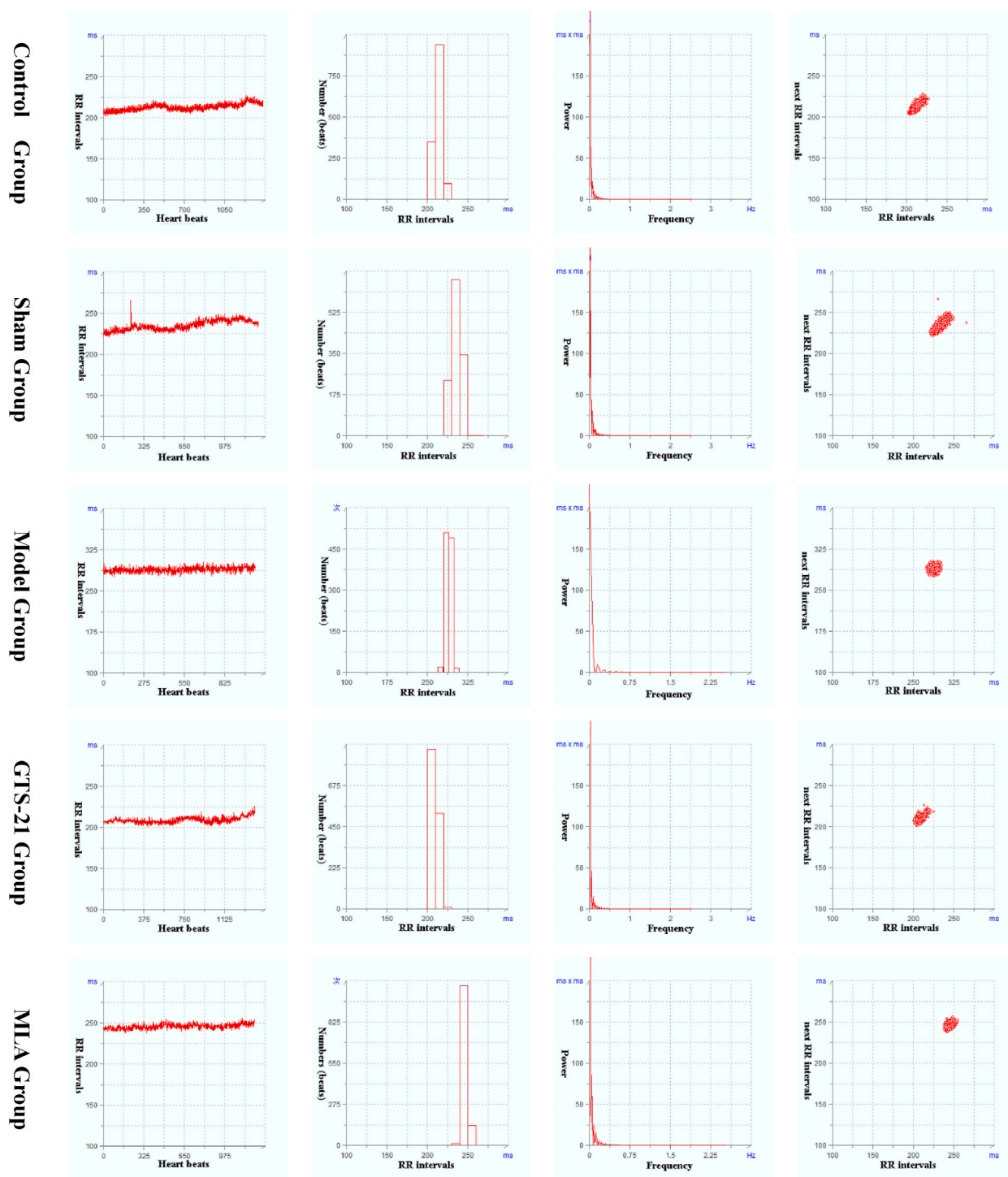


Fig. 1. Some representative diagrams of heart rate variability with time domain, frequency domain and non-linear analysis from each group.

minimal changes observed in the Spectrogram among the five groups. However, in the Lorenz Scatter plot (a nonlinear analysis that includes SD1 and SD2), the scatter plot distributions appeared more rounded (indicating SD1 was approximately equal to SD2) in the Model Group and MLA Group as compared to the Control Group, Sham Group, and GTS-21 Group.

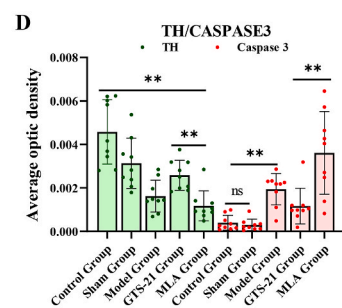
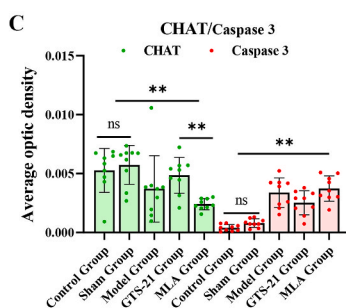
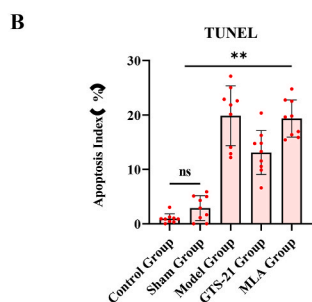
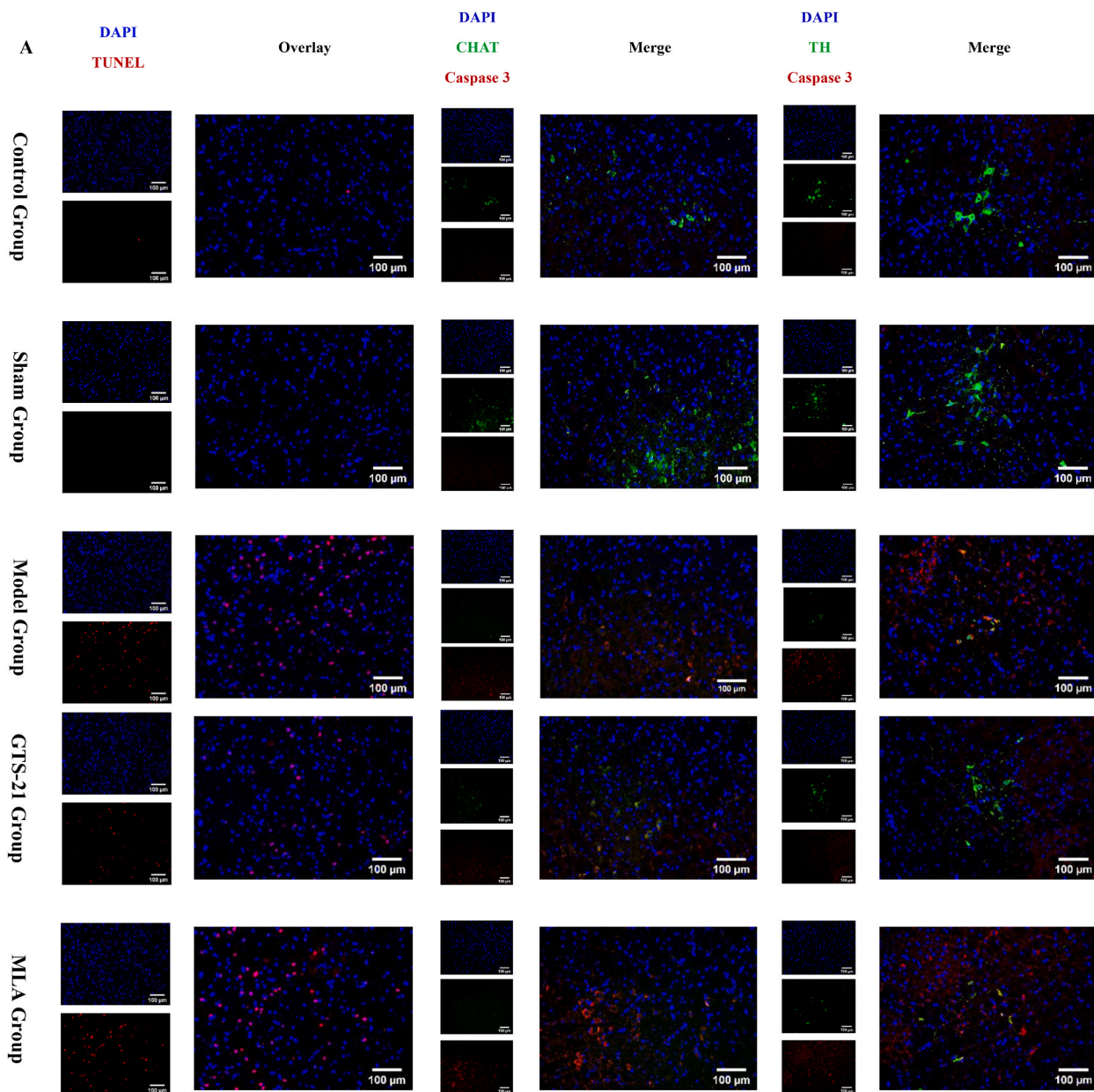


Fig. 2. Pathological changes of MVZ in sepsis and intervened by cholinergic anti-inflammatory pathway (TUNEL and double immunofluorescence labeling experiments).

3.3. The pathological changes of MVZ

The TUNEL analysis revealed that the Septic Groups, including the MLA Group, Model Group and GTS-21 Group exhibited significantly higher levels of apoptotic neurons compared to the Control Groups ($29.11 \pm 4.60\%$, $25.40 \pm 9.13\%$, $17.03 \pm 4.16\%$ vs $5.30 \pm 0.9\%$, $P = 0.000$, $P = 0.000$, $P = 0.000$). GTS-21 Group showed a tendency to reduce apoptosis compared to the Model Group ($P = 0.074$) (Fig. 2 Part A, B).

The double-labeling fluorescence analysis showed that the expression of TH significantly decreased in the MLA Group, Model Group and GTS-21 Group compared to the Control Group (0.00117 ± 0.00069 , 0.00162 ± 0.00073 , 0.00258 ± 0.00069 vs 0.00458 ± 0.00148 , $P = 0.000$, $P = 0.000$, $P = 0.001$). While GTS-21 tended to upregulate the expression of TH in model rats, MLA further reduced it remarkably compared to GTS-21 Group ($P = 0.488$, $P = 0.048$). However, the expression of CHAT did not significantly decrease in the Model Group and GTS-21 Group, while in the MLA Group, it reduced significantly compared to the Control Group (0.00370 ± 0.00282 , 0.00485 ± 0.00151 , 0.00241 ± 0.00047 vs 0.00527 ± 0.00186 , $P = 0.761$, $P = 1.000$, $P = 0.019$). The expression of Caspase3 was evidently up-regulated in the MLA Group, Model Group and GTS-21 Group when compared to the Control Group (0.00373 ± 0.00107 , 0.00338 ± 0.00125 , 0.00253 ± 0.00102 vs 0.00039 ± 0.00028 , $P = 0.000$, $P = 0.000$, $P = 0.000$), GTS-21 showing a tendency to curb its expression, while MLA boosted its expression (Fig. 2 Part A, C, D).

Fig. 2 illustrates the impact of sepsis on MVZ neurons, including cholinergic and catecholaminergic neurons, in terms of apoptosis and inactivity.

Part A of the figure displays TUNEL and double immunofluorescence labeling images of MVZ. The red fluorescence in the TUNEL column indicates apoptotic cells. In the TH/Caspase3 column, green fluorescence represents the expression of TH, while red fluorescence indicates the expression of caspase 3 in catecholaminergic neurons. In the CHAT/Caspase3 column, green fluorescence represents the expression of CHAT, and red fluorescence shows the expression of caspase 3 in cholinergic neurons. These images reveal that sepsis not only induces significant apoptosis of catecholaminergic and cholinergic neurons in MVZ, but also affects their activity. Intervention with the cholinergic anti-inflammatory pathway can impact the activity and apoptosis of functional neurons in the MVZ area. The $\alpha 7$ nAChR agonist GTS-21 tends to prevent apoptosis and inactivity of cholinergic and catecholaminergic neurons in MVZ, while the $\alpha 7$ nAChR antagonist MLA significantly accelerates apoptosis and inactivity of these two types of neurons.

Part B of the figure presents a histogram of TUNEL analysis, confirming that sepsis induces significant apoptosis in MVZ, and activation of the cholinergic anti-inflammatory pathway tends to reverse it, while blocking the pathway exacerbates apoptosis.

Part C of the figure shows a histogram of TH/Caspase3 expressions in MVZ, indicating that sepsis causes significant apoptosis of catecholaminergic neurons in MVZ. GTS-21 can reverse this situation, whereas MLA has the opposite effect. In addition, both sepsis and sham operation lead to significantly low expression of TH, especially when rats are treated with MLA.

Part D of the figure displays a histogram of CHAT/Caspase3 expressions in MVZ, revealing that although sepsis induces significant apoptosis of cholinergic neurons in MVZ, it does not significantly reduce the expression of CHAT, except in the MLA Group.

** $: P < 0.01$; ns: $P > 0.05$.

3.4. The key genes' expressions in MVZ in sepsis and interfered by CAP

RT-PCR analysis revealed that sepsis led to increased expressions of GFAP mRNA, MMP-9 mRNA, and decreased expression of Olig-2 mRNA in the MLA Group, Model Group and GTS-21 Group compared to the Control Group (3.756 ± 0.726 , 2.825 ± 0.750 , 1.676 ± 0.420 vs 1.071 ± 0.195 , $P = 0.000$, $P = 0.000$, $P = 0.195$; 3.949 ± 0.724 , 3.169 ± 0.702 , 2.043 ± 0.361 vs 1.073 ± 0.194 , $P = 0.000$, $P = 0.000$, $P = 0.002$; 0.232 ± 0.061 , 0.534 ± 0.136 , 0.719 ± 0.143 vs 1.027 ± 0.189 , $P = 0.000$, $P = 0.000$, $P = 0.001$). Intervention with

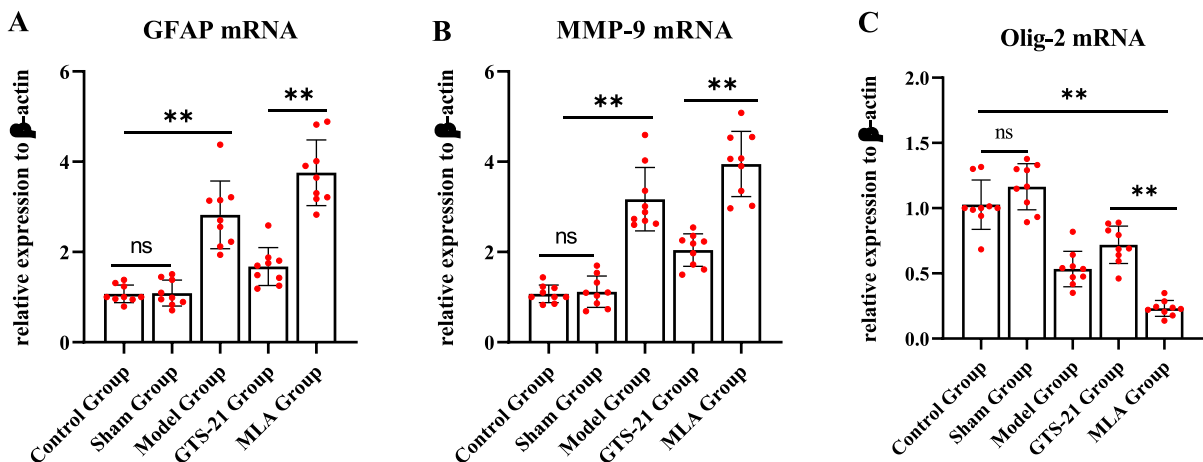


Fig. 3. The expressions of key genes in MVZ in sepsis and interfered by CAP.

CAP significantly influenced these gene expression changes. GTS-21 treatment was found to significantly reverse these gene expression changes, indicating that activation of CAP promotes the normalization of gene expressions in MVZ. On the other hand, blocking CAP with MLA resulted in opposite effects (Fig. 3).

Using GAPDH as an internal reference, it was observed that sepsis resulted in simultaneous up-regulation of GFAP mRNA (Part A) and MMP-9 mRNA expression (Part B), and down-regulation of Olig-2 mRNA expression (Part C). Treatment with GTS-21 reversed these changes, while MLA had the opposite effect.

3.5. Inflammatory cytokines expression in MVZ and serum among different groups

The expression levels of TNF-a and IL-6 in MVZ induced by sepsis were significantly increased, and central anti-inflammation by minocycline significantly reduced the expression levels of TNF-a and IL-6 in MVZ induced by sepsis. However, right vagotomy abolished the central anti-inflammatory effect by minocycline, resulting in apparently increased expression of TNF-a and IL-6 in MVZ in CAP Transection Groups, see Fig. 4 A-C.

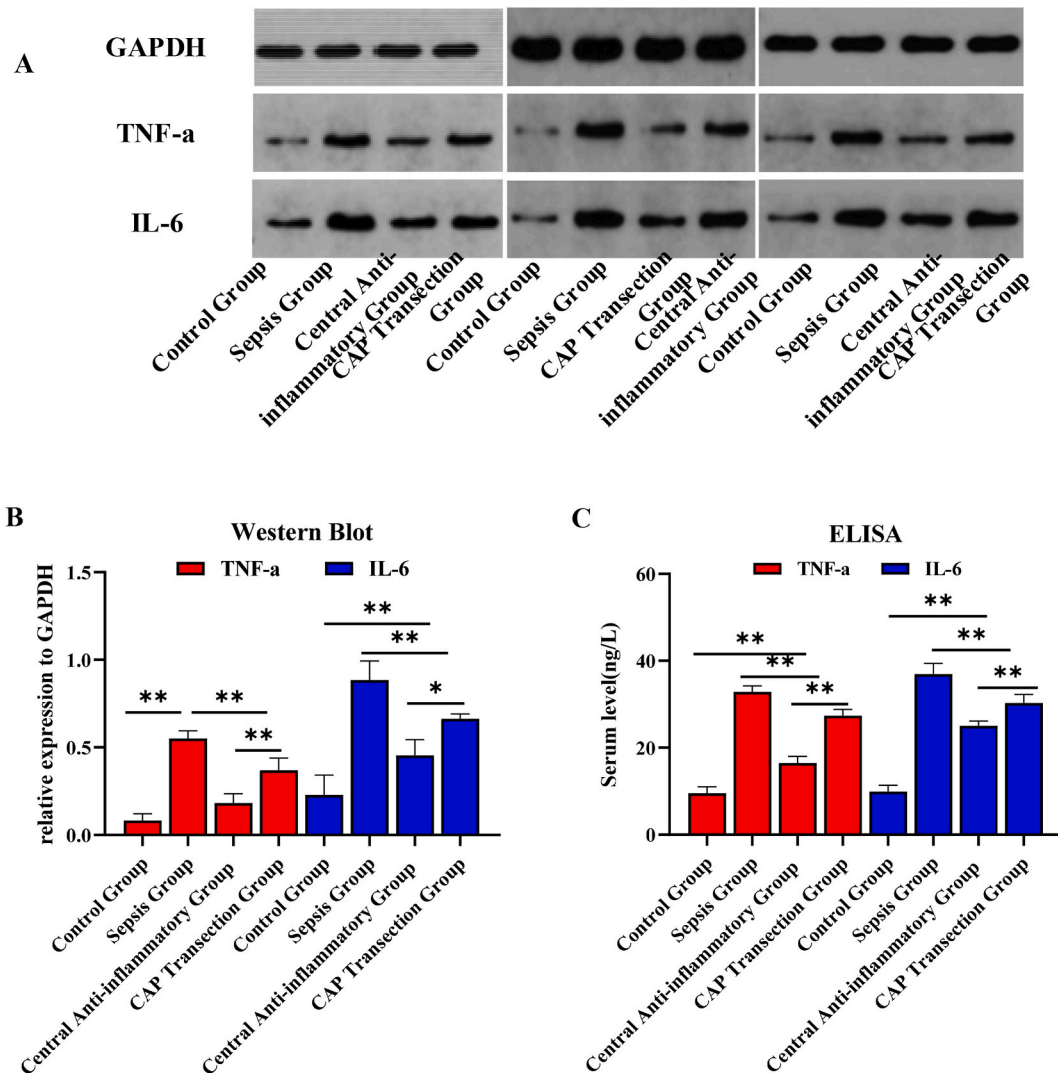


Fig. 4. Inflammatory cytokines expression in MVZ and serum among different groups Part A: the images of WB of TNF-a and IL-6 expressions in MVZ, the Bar charts of Part B illustrate the comparison of TNF-a and IL-6 expression among four groups. They demonstrated that the inflammatory cytokines in the Sepsis Group were significantly higher than those in the Control Group (TNF-a: 0.551 ± 0.044 vs 0.083 ± 0.039 , $P = 0.000$; IL-6: 0.885 ± 0.108 vs 0.229 ± 0.113 , $P = 0.000$). Whereas, in the Central Anti-inflammatory Group, these cytokines were significantly dampened compared to those of the Model Group (TNF-a: 0.181 ± 0.054 vs 0.551 ± 0.044 , $P = 0.000$; IL-6: 0.454 ± 0.091 vs 0.885 ± 0.108 , $P = 0.000$). The declination of cytokines by minocycline's anti-inflammation in MVZ was obviously reversed by the right vagotomy (TNF-a: 0.370 ± 0.069 vs 0.181 ± 0.054 , $P = 0.002$; IL-6: 0.664 ± 0.026 vs 0.454 ± 0.091 , $P = 0.023$). The expression of TNF-a in the Central Anti-inflammatory Group was not significantly different from that in the Control Group ($P = 0.051$).

The serum levels of TNF- α , IL-6 in sepsis models were significantly increased, and central anti-inflammation by minocycline significantly reduced the serum levels of TNF- α , IL-6 in these two model rats. However, right vagotomy abolished the central anti-inflammatory effect, resulting in significant increase of serum TNF- α , IL-6 in the rats of CAP Transection Group, refer to Fig. 4 D, E.

The Bar charts of Part C illustrate the comparison of TNF- α and IL-6 serum levels among four groups. They demonstrated that The serum concentration of inflammatory cytokines in the Sepsis Group were significantly higher than those in the Control Group [TNF- α (ng/L): 32.84 ± 1.39 vs 9.51 ± 1.50 , $P = 0.000$; IL-6 (ng/L): 36.94 ± 2.50 vs 9.94 ± 1.44 , $P = 0.000$]; They decreased significantly in the Central Anti-inflammatory Group compared to the Model Group [TNF- α (ng/L): 16.46 ± 1.55 vs 32.84 ± 1.39 , $P = 0.000$; IL-6 (ng/L): 25.01 ± 1.13 vs 36.94 ± 2.50 , $P = 0.000$], whereas, in the Vagus Transection Group, they had marvelous rebounds compared to the Central Anti-inflammatory Group [TNF- α (ng/L): 27.36 ± 1.48 vs 16.46 ± 1.55 , $P = 0.000$; IL-6 (ng/L): 30.30 ± 1.91 vs 25.01 ± 1.13 , $P = 0.007$].

** $: P < 0.01$.

4. Discussion

Building upon our previous research, the findings of this study provide valuable insights. We can reasonably speculate that sepsis causes neuroinflammation in MVZ, resulting in inflammatory demyelination which underlies decreased tone of the vagus nerve and emergence of systemic inflammatory response syndrome. Although pharmacological intervention targeting CAP partially modifies MVZ neuron apoptosis and function, these chemicals have minimal effect on CAP's modulation of systemic inflammation intensity in sepsis.

The cholinergic anti-inflammatory pathway (CAP), predominantly controlled by the MVZ, plays a negative regulatory role in systemic inflammation induced by sepsis.

The vagus nerve (VN) exerts rapid and precise control over systemic inflammation through CAP [34]. By modulating the release of acetylcholine (ACh), CAP can effectively adjust the intensity of systemic inflammation in response to the body's needs. Upon acting on $\alpha 7nAChR$ of innate immune cells, such as monocytes, ACh inhibits the activation of Toll-like receptor 4 (TLR4) signaling, thereby stabilizing innate immune cells and reducing their release of pro-inflammatory cytokines [35,36]. In essence, CAP dynamically, efficiently, and precisely regulates systemic inflammation in a negative manner [37,38]. Clearly, the structural and functional integrity of MVZ, as the commander of CAP, is crucial in sepsis.

Our previous studies have confirmed that CAP exerts a negative regulatory effect on systemic inflammation induced by sepsis [12]. Treatment with GTS-21, a specific agonist of $\alpha 7nAChR$, significantly reduces serum levels of inflammatory mediators such as TNF- α , IL-1 α , IL-6, IL-10, sCD14, and HMGB1, and inhibits immune activation in sepsis. In contrast, treatment with MLA, a specific antagonist of $\alpha 7nAChR$, produces opposite effects.

The potential central effects of CAP, particularly on the function and pathology of MVZ, remain unclear. Both GTS-21 and MLA are capable of crossing the blood-brain barrier, and they may also interact with central $\alpha 7nAChRs$, which are widely expressed in the mammalian brain, including microglia and astrocytes [39,40]. Activation of $\alpha 7nAChRs$ can significantly inhibit neuroinflammation. Therefore, interfering with CAP may also impact the strength of neuroinflammation. Considering that neuroinflammation is known to play a crucial role in suppressing neuronal function and remodeling neural structure through oxidative stress [41], it is possible that neuroinflammation in MVZ may dysregulate CAP.

Sepsis results in apoptosis and suppression of cholinergic and catecholaminergic neurons in MVZ, and intervention of CAP can modify these pathologies.

Previous studies have shown that peripheral VN stimulation through CAP has a definite effect in suppressing neuroinflammation and promoting neural function recovery in various CNS diseases [42]. Therefore, it can be reasonably deduced that CAP may regulate inflammation and function of MVZ in sepsis. In this study, TUNEL and fluorescence double-labeling analysis revealed evident apoptosis of both cholinergic and catecholaminergic neurons in sepsis, indicating MVZ damage. The reduced expression of TH suggests suppression of catecholaminergic neurons, while the expression of CHAT remained statistically unchanged except in the MLA Group, possibly indicating that cholinergic neurons were excited by systemic inflammation and synthesize acetylcholine to enhance CAP's function to curb peripheral inflammation in sepsis, unless severely damaged in the MLA Group. Caspase 3 is a known indicator of neuronal apoptosis, especially in ischemia-reperfusion injuries [43]. Cerebral injuries induced by sepsis also involve damage to the Blood Brain Barrier, neuroinflammation, and Oxidative Stress, which can activate the mitochondrial apoptotic pathway characterized by increased caspase 3 and caspase 9, and BCL2-Associated X/B-cell lymphoma-2 ratio [44]. Therefore, Caspase 3 can serve as a reliable indicator of neuronal apoptosis induced by sepsis. Therefore, sepsis induces apoptosis and suppression of pivotal neurons in MVZ. Considering our previous study [45], we reasonably deduced that intervention of CAP not only alters the levels of systemic inflammation and immunity, but also has a significant impact on MVZ in sepsis, which may profoundly affect the output of CAP.

MVZ is primarily composed of the Nucleus Tractus Solitarius (NTS), Rostral Ventrolateral Medulla (RVLM), and Vagus Dorsal Motor Nucleus (VDMN). RVLM contains abundant catecholamine neurons that not only bridge the sympathetic and parasympathetic systems, but also connect the autonomic nervous system with the hypothalamic-pituitary-adrenal (HPA) axis, as well as the afferent and efferent systems of VN, coordinating the regulation of systemic inflammation [46]. Cholinergic neurons in VDMN are known to negatively regulate innate immunity through CAP [47]. The apoptosis or inactivity of catecholaminergic and cholinergic neurons in MVZ can inevitably impact the modulation of systemic inflammation and immunity. The vitality of cholinergic neurons is directly related to the modulation of systemic inflammation through CAP, while the vitality of catecholaminergic neurons indirectly influences the modulation of systemic inflammation through CAP. Therefore, functional stabilization of cholinergic neurons is critical for the modulation of systemic inflammation.

Sepsis induces suppression of CAP, as suggested by the reduction of certain indicators of heart rate variability (HRV). However, intervention of CAP has minimal influence on HRV in sepsis.

As our previous study [12], certain HRV parameters such as SDNN, RMSSD, HF, SD1, SD2 are more reliable in reflecting the regulatory effect of CAP. It was anticipated that these parameters would significantly increase in the GTS-21 Group if the output of CAP was enhanced by GTS-21, and vice versa for the MLA Group where these parameters would show a significant reduction. HRV analysis would provide insights into the actual effect.

In this study, we observed that some HRV parameters, including SDNN, RMSSD, HF, SD1, SD2, were significantly reduced in all three Septic Groups compared to the Control Group, indicating inhibition of CAP in sepsis. However, these parameters did not show significant difference in the three Septic Groups. This suggests that the output of CAP was not elevated by GTS-21, and it was not lowered by MLA in sepsis, which is inconsistent with our previous anticipation.

As mentioned previously, it was expected that the functional stabilization of cholinergic neurons in sepsis would effectively modulate CAP. However, in our experiment, in spite that cholinergic neurons possess strong compensatory functions in sepsis, the results indicate that intervention of CAP had minimal influence on HRV in sepsis. It is consistent with the findings of Pinto's research [48] that the intensity of neuroinflammation in the autonomic center is not correlated with HRV in sepsis. Although there were significant differences in the apoptosis of MVZ neurons among the three Septic Groups, there was minimal variation in vagal nerve tension, indicating that transmission of neural commands to CAP in sepsis was impaired.

Neuroinflammation, gliosis, and remodeling of extracellular matrix coexist in the MVZ during sepsis, and inflammatory demyelination of MVZ is associated with CAP's inhibition.

Pro-inflammatory cytokines such as TNF- α , IL-6, and IL-1 β in the central nervous system (CNS) can activate microglia during systemic inflammation [49]. Similar to many previous studies [50,51], our study confirmed that sepsis induces neuroinflammation in the MVZ. Neuroinflammation and apoptosis promote the expressions of GFAP mRNA, MMP-9 mRNA [52,53], which suggest nerve injury, gliosis, and remodeling of extracellular matrix [54–57]. Oligodendrocyte Transcription Factor 2 (Olig-2) is a marker of oligodendrocytes [58,59], which are myelin-forming cells that ensure rapid conduction of neural information. Therefore, the down-regulation of Olig2 mRNA in the Septic Group indicates insufficient and damaged myelination of nerve fibers. Myelination damage of nerve fibers leads to obstacles in regulatory signals transmitting to the periphery, equivalent to almost transection of CAP. In the early stages of neuroinflammation, MMP-9 damages the blood-brain barrier, degrades myelin basic protein, promotes the secretion of inflammatory factors, initiates inflammatory cascades, and directly or indirectly promotes demyelination [60]. The up-regulated expression of GFAP denotes exacerbation of inflammation and gliosis, while the up-regulated expression of Olig-2 hints at the remission of inflammation and the initiation of nerve repair.

Our study demonstrates that the activation of CAP (GTS-21 Group) dampens neuroinflammation and promotes the normalization of MVZ, whereas the suppression of CAP (MLA Group) has the opposite effect. Most importantly, according to these results, we speculate that sepsis results in inflammatory demyelination in MVZ, which is associated with CAP inhibition in early sepsis. Inflammatory demyelination of MVZ plays a key role in the uncontrolled systemic inflammatory storm in early sepsis and should be a target for the treatment of severe sepsis.

CNS undergoes continuous demyelination and remyelination throughout adulthood [61]. Maintaining a dynamic balance between demyelination and remyelination is crucial for preventing neural degeneration and restoring CNS physiological function. Neuroinflammation can activate microglia and result in excessive production of proinflammatory mediators such as IL-1 β , which can damage oligodendrocytes, axons, and lead to myelin destruction [62], ultimately impairing neural information transmission [63]. Therefore, the impact of demyelination of nerve fibers is equivalent to partial or complete transection of the neural stem. Inflammatory demyelination in MVZ should receive greater attention in the clinical practice of sepsis.

This study has certain limitations. The intervention in this study only focuses on the VN and does not reflect the regulatory effect of the sympathetic nerve on inflammation and immunity. Therefore, the interpretation of some HRV indicators may be inaccurate or even incorrect. Additionally, the output of CAP is not directly measured by the device, but is rather deduced indirectly from some HRV indexes, which may be unreliable or inaccurate. Lastly, this study is an animal experiment and clinical studies may yield different results, requiring further investigation in clinical practice.

5. Conclusions

In conclusion, neuroinflammation in MVZ affected systemic inflammation through CAP in sepsis. Inflammatory demyelination of MVZ resulted in CAP's dysfunction and systemic inflammatory response syndrome and should be a target in sepsis.

Funding statement

This study was supported by the Key Projects of Guizhou Provincial Science and Technology Foundation (No. ZK [2023]key-001), the Science and Technology Fund of Guizhou Provincial Health Commission (No. gzwkj2021-001), and the Guizhou Provincial Science and Technology Foundation (No. [2019]1005).

Data availability

As this study is supported by the Guizhou Provincial Science and Technology Foundation and the Science and Technology Fund of Guizhou Provincial Health Commission, the data will not be made public until the research project has been checked and accepted.

Therefore, we haven't deposited the data associated with our study into a publicly available repository. All datasets used and/or analyzed during the current study are available from the authors upon reasonable request. The email address for requesting the data is mrbright789@sina.com.

Consent for publication

The authors declare that there is no conflict of interest regarding the publication of this paper.

Ethics approval and consent to participate

All experimental protocols were conducted in accordance with the Guidance Suggestions for the Care and Use of Laboratory Animals formulated by the Ministry of Science and Technology of the People's Republic of China (2006 Edition). The study was reviewed and approved by the Ethics Committee of the First Hospital of Guiyang, Guizhou Province, China (Approval No.: 20190107).

CRediT authorship contribution statement

Gao Chen: Investigation, Data curation, Conceptualization. **Cheng Zhang:** Writing – original draft, Methodology, Investigation, Conceptualization. **Hongbing Li:** Writing – review & editing, Investigation, Funding acquisition, Conceptualization. **Xian Liu:** Writing – review & editing, Writing – original draft, Validation, Formal analysis, Data curation.

Declaration of competing interest

The authors declare the following financial interests/personal relationships which may be considered as potential competing interests: Hongbing Li reports financial support was provided by the Key Projects of Guizhou Provincial Science and Technology Foundation. Hongbing Li reports financial support was provided by the Science and Technology Fund of Guizhou Provincial Health Commission. Hongbing Li reports financial support was provided by the Guizhou Provincial Science and Technology Foundation. If there are other authors, they declare that they have no known competing financial interests or personal relationships that could have appeared to influence the work reported in this paper.

Acknowledgements

Not applicable.

Appendix A. Supplementary data

Supplementary data to this article can be found online at <https://doi.org/10.1016/j.heliyon.2024.e33840>.

References

- [1] S. Oczkowski, F. Alshamsi, E. Belley-Cote, et al., Surviving sepsis Campaign guidelines 2021: highlights for the practicing clinician, *Pol. Arch. Intern. Med.* 132 (7–8) (2022) 16290.
- [2] S. Weis, A.R. Carlos, M.R. Moita, et al., Metabolic adaptation establishes disease tolerance to sepsis, *Cell* (7) (2017) 169.
- [3] K.J. Tracey, Reflex control of immunity, *Nat. Rev. Immunol.* 9 (6) (2009) 418–428.
- [4] L. Yue-Chun, X.H. Gu, G. Li-Sha, et al., Vagus nerve plays a pivotal role in CD4+ T cell differentiation during CVB3-induced murine acute myocarditis, *Virulence* 12 (1) (2021) 360–376.
- [5] L. Yue-Chun, X.H. Gu, G. Li-Sha, et al., Vagus nerve plays a pivotal role in CD4+ T cell differentiation during CVB3-induced murine acute myocarditis, *Virulence* 12 (1) (2021) 360–376.
- [6] V.A. Pavlov, K.J. Tracey, Neural regulation of immunity: molecular mechanisms and clinical translation, *Nat. Neurosci.* 20 (2) (2017) 156–166.
- [7] P. Saunders, A.W. Horne, Endometriosis: etiology, pathobiology, and therapeutic prospects, *Cell* 184 (11) (2021) 2807–2824.
- [8] X. Xie, N. Zhang, J. Fu, et al., The potential for traditional Chinese therapy in treating sleep disorders caused by COVID-19 through the cholinergic anti-inflammatory pathway, *Front. Pharmacol.* 10 (13) (2022) 1009527, <https://doi.org/10.3389/fphar.2022.1009527>.
- [9] M.D. Okusa, D.L. Rosin, K.J. Tracey, Targeting neural reflex circuits in immunity to treat kidney disease, *Nat. Rev. Nephrol.* 13 (11) (2017) 669–680.
- [10] R. Sassi, S. Cerutti, F. Lombardi, M. Malik, H.V. Huikuri, C.K. Peng, G. Schmidt, Y. Yamamoto, Advances in heart rate variability signal analysis: joint position statement by the e-cardiology ESC working group and the European heart rhythm association co-endorsed by the asia pacific heart rhythm society, *Journal of the working groups on cardiac pacing, arrhythmias, and cardiac cellular electrophysiology of the European Society of Cardiology* 17 (9) (2015) 1341–1353, <https://doi.org/10.1093/europace/euv015>. Europace : European pacing, arrhythmias, and cardiac electrophysiology.
- [11] B. Goldstein, D.H. Fiser, M.M. Kelly, D. Mickelsen, U. Ruttimann, M.M. Pollack, Decomplexification in critical illness and injury: relationship between heart rate variability, severity of illness, and outcome, *Crit. Care Med.* 26 (2) (1998) 352–357, <https://doi.org/10.1097/00003246-199802000-00040>.
- [12] H.B. Li, Y. Zhou, A.H. Zhao, L.L. Guo, Exploring the mechanism on the medullary visceral zone inhibiting the cholinergic anti-inflammatory pathway induced by sepsis, *Mediat. Inflamm.* 2020 (2020) 1320278, <https://doi.org/10.1155/2020/1320278>.
- [13] V.A. Pavlov, K.J. Tracey, Neural regulation of immunity: molecular mechanisms and clinical translation, *Nat. Neurosci.* 20 (2) (2017) 156–166, <https://doi.org/10.1038/nn.4477>.
- [14] L. Zhang, F. Xiao, J. Zhang, et al., Dexmedetomidine mitigated NLRP3-mediated neuroinflammation via the ubiquitin-autophagy pathway to improve perioperative neurocognitive disorder in mice, *Front. Pharmacol.* 12 (2021) 1143.

- [15] S.J. Kim, M.J. Ryu, J. Han, Y. Jang, J. Kim, M.J. Lee, I. Ryu, X. Ju, E. Oh, W. Chung, G.R. Kweon, J.Y. Heo, Activation of the HMGB1-RAGE axis upregulates TH expression in dopaminergic neurons via JNK phosphorylation, *Biochem. Biophys. Res. Commun.* 493 (1) (2017) 358–364, <https://doi.org/10.1016/j.bbrc.2017.09.017>.
- [16] Z. Nahla, M.E. Addorisio, H.A. Silverman, et al., Forebrain cholinergic dysfunction and systemic and brain inflammation in murine sepsis survivors, *Front. Immunol.* 8 (2017) 1673.
- [17] J. Zhang, Y. Zheng, Y. Wang, J. Wang, A. Sang, X. Song, X. Li, YAP1 alleviates sepsis-induced acute lung injury via inhibiting ferritinophagy-mediated ferroptosis, *Front. Immunol.* 13 (2022 Aug 1) 884362, <https://doi.org/10.3389/fimmu.2022.884362>.
- [18] H.B. Li, W.B. Liang, L. Zhou, The experimental research on neuroplasticity in rats' hippocampus subjected to chronic cerebral hypoperfusion and interfered by Modified Dioscorea Pills, *Heliyon* 6 (1) (2019) e02897, <https://doi.org/10.1016/j.heliyon.2019.e02897>.
- [19] W.H. Zhou, J.G. Li, Establishment of sepsis and cholinergic anti-inflammatory pathway model, *Med. J. Wuhan Univ.* 37 (5) (2016) 748–751.
- [20] Z. Miao, Y. Wang, J. Tian, Y. Ding, Mechanism of cognitive impairment by $\alpha 7$ nAChR competitive antagonist methyllycaconitine in mouse, *Chin. J. Anat.* 33 (6) (2010) 764–767.
- [21] M.N. Jarczok, J. Koenig, A. Wittling, J.E. Fischer, J.F. Thayer, First evaluation of an Index of low vagally-mediated heart rate variability as a marker of health risks in human adults: proof of concept, *J. Clin. Med.* 8 (11) (2019) 1940, <https://doi.org/10.3390/jcm8111940>.
- [22] C.M. Badke, L.E. Marsillio, D.E. Weese-Mayer, L.N. Sanchez-Pinto, Autonomic nervous system dysfunction in pediatric sepsis, *Frontiers in pediatrics* 6 (2018) 280, <https://doi.org/10.3389/fped.2018.00280>.
- [23] L. Wu, Z. Jiang, C. Li, M. Shu, Prediction of heart rate variability on cardiac sudden death in heart failure patients: a systematic review, *Int. J. Cardiol.* 174 (3) (2014) 857–860, <https://doi.org/10.1016/j.ijcard.2014.04.176>.
- [24] I.T. Fonkoue, P.J. Marvar, S. Norrholm, Y. Li, M.L. Kankam, T.N. Jones, M. Vemulapalli, B. Rothbaum, J.D. Bremner, N.A. Le, J. Park, Symptom severity impacts sympathetic dysregulation and inflammation in post-traumatic stress disorder (PTSD), *Brain Behav. Immun.* 83 (2020) 260–269.
- [25] F.A. Koopman, S.S. Chavan, S. Miljko, S. Grazio, S. Sokolovic, P.R. Schuurman, A.D. Mehta, Y.A. Levine, M. Faltys, R. Zitnik, K.J. Tracey, P.P. Tak, Vagus nerve stimulation inhibits cytokine production and attenuates disease severity in rheumatoid arthritis, *Proc. Natl. Acad. Sci. U.S.A.* 113 (29) (2016) 8284–8289, <https://doi.org/10.1073/pnas.1605635113>.
- [26] M.I. Samsudin, N. Liu, S.M. Prabhakhar, S.L. Chong, W. Kit Lye, Z.X. Koh, D. Guo, R. Rajesh, A. Ho, M. Ong, A novel heart rate variability based risk prediction model for septic patients presenting to the emergency department, *Medicine* 97 (23) (2018) e10866, <https://doi.org/10.1097/MD.00000000000010866>.
- [27] J.C. Bonjorno Junior, F.R. Caruso, R.G. Mendes, T.R. da Silva, T. Biazon, F. Rangel, S.A. Phillips, R. Arena, A. Borghi-Silva, Noninvasive measurements of hemodynamic, autonomic and endothelial function as predictors of mortality in sepsis: a prospective cohort study, *PLoS One* 14 (3) (2019) e0213239, <https://doi.org/10.1371/journal.pone.0213239>.
- [28] D.P. Barnaby, S.M. Fernando, K.J. Ferrick, C.L. Herry, A. Seely, P.E. Bijur, E.J. Gallagher, Use of the low-frequency/high-frequency ratio of heart rate variability to predict short-term deterioration in emergency department patients with sepsis, *Emerg. Med. J. : Eng. Manag. J.* 35 (2) (2018) 96–102, <https://doi.org/10.1136/emermed-2017-206625>.
- [29] K.B. Min, J.Y. Min, D. Paek, S.I. Cho, M. Son, Is 5-minute heart rate variability a useful measure for monitoring the autonomic nervous system of workers? *Int. Heart J.* 49 (2) (2008) 175–181, <https://doi.org/10.1536/ihj.49.175>.
- [30] A. Sgoifo, D. Stilli, D. Medici, P. Gallo, B. Aimi, E. Musso, Electrode positioning for reliable telemetry ECG recordings during social stress in unrestrained rats, *Physiol. Behav.* 60 (6) (1996) 1397–1401, [https://doi.org/10.1016/s0031-9384\(96\)00228-4](https://doi.org/10.1016/s0031-9384(96)00228-4).
- [31] Y. Lei, Y. Zhen, W. Zhang, X. Sun, X. Lin, J. Feng, H. Luo, Z. Chen, C. Su, B. Zeng, J. Chen, Exogenous hydrogen sulfide exerts proliferation, anti-apoptosis, angiopoiesis and migration effects via activating HSP90 pathway in EC109 cells, *Oncol. Rep.* 35 (6) (2016) 3714–3720, <https://doi.org/10.3892/or.2016.4734>.
- [32] L. da Costa, N. Júnior, C. Catalão, T. Sharshar, F. Chrétien, M. da Rocha, Vasopressin impairment during sepsis is associated with hypothalamic intrinsic apoptotic pathway and microglial activation, *Mol. Neurobiol.* 54 (7) (2017) 5526–5533, <https://doi.org/10.1007/s12035-016-0094-x>.
- [33] W. Yang, J.G. Wang, J. Xu, D. Zhou, K. Ren, C. Hou, L. Chen, X. Liu, HCRP1 inhibits TGF- β induced epithelial-mesenchymal transition in hepatocellular carcinoma, *Int. J. Oncol.* 50 (4) (2017) 1233–1240, <https://doi.org/10.3892/ijo.2017.3903>.
- [34] K.J. Tracey, Reflexes in immunity, *Cell* 164 (3) (2016) 343–344, <https://doi.org/10.1016/j.cell.2016.01.018>.
- [35] K.J. Tracey, Reflex control of immunity, *Nat. Rev. Immunol.* 9 (6) (2009) 418–428, <https://doi.org/10.1038/nri2566>.
- [36] C. Zhao, X. Yang, E.M. Su, Y. Huang, L. Li, M.A. Matthay, X. Su, Signals of vagal circuits engaging with AKT1 in $\alpha 7$ nAChR+CD11b+ cells lessen E. coli and LPS-induced acute inflammatory injury, *Cell discovery* 3 (2017) 17009, <https://doi.org/10.1038/celldisc.2017.9>.
- [37] F.M. Santos-Almeida, G. Domingos-Souza, C.A. Meschiar, L.C. Fávaro, C. Becari, J.A. Castania, A. Lopes, T.M. Cunha, D. Moraes, F.Q. Cunha, L. Ulloa, A. Kanashiro, G. Tezini, H.C. Salgado, Carotid sinus nerve electrical stimulation in conscious rats attenuates systemic inflammation via chemoreceptor activation, *Sci. Rep.* 7 (1) (2017) 6265, <https://doi.org/10.1038/s41598-017-06703-0>.
- [38] G.S. Bassi, D. Dias, M. Franchin, J. Talbot, D.G. Reis, G.B. Menezes, J.A. Castania, N. Garcia-Cairasco, L. Resstel, H.C. Salgado, F.Q. Cunha, T.M. Cunha, L. Ulloa, A. Kanashiro, Modulation of experimental arthritis by vagal sensory and central brain stimulation, *Brain Behav. Immun.* 64 (2017) 330–343, <https://doi.org/10.1016/j.bbi.2017.04.003>.
- [39] O.K. Steinlein, D. Bertrand, Neuronal nicotinic acetylcholine receptors: from the genetic analysis to neurological diseases, *Biochem. Pharmacol.* 76 (10) (2008) 1175–1183, <https://doi.org/10.1016/j.bcp.2008.07.012>.
- [40] Q. Zhang, Y. Lu, H. Bian, L. Guo, H. Zhu, Activation of the $\alpha 7$ nicotinic receptor promotes lipopolysaccharide-induced conversion of M1 microglia to M2, *Am. J. Tourism Res.* 9 (3) (2017) 971–985.
- [41] K. Wu, C.W. Wu, Y.M. Chao, C.Y. Hung, J. Chan, Impaired Nrf2 regulation of mitochondrial biogenesis in rostral ventrolateral medulla on hypertension induced by systemic inflammation, *Free Radic. Biol. Med.* 97 (2016) 58–74.
- [42] K. Duris, J. Lipkova, M. Jurajda, Cholinergic anti-inflammatory pathway and stroke, *Curr. Drug Deliv.* 14 (4) (2017) 449–457, <https://doi.org/10.2174/1567201814666170201150015>.
- [43] Z.Q. Shao, S.S. Dou, J.G. Zhu, H.Q. Wang, C.M. Wang, B.H. Cheng, B. Bai, Apelin-13 inhibits apoptosis and excessive autophagy in cerebral ischemia/reperfusion injury, *Neural regeneration research* 16 (6) (2021) 1044–1051, <https://doi.org/10.4103/1673-5374.300725>.
- [44] M. Gu, X.L. Mei, Y.N. Zhao, Sepsis and cerebral dysfunction: BBB damage, neuroinflammation, oxidative stress, apoptosis and autophagy as key mediators and the potential therapeutic approaches, *Neurotox. Res.* 39 (2) (2021) 489–503, <https://doi.org/10.1007/s12640-020-00270-5>.
- [45] H. Li, Y. Li, W. Wang, Z. Peng, F. Wu, Cholinergic anti-inflammatory pathway plays negative regulatory role in early inflammatory and immune responses in septic rats, *J. South. Med. Univ.* 40 (5) (2020) 647–653, <https://doi.org/10.12122/j.issn.1673-4254.2020.05.06>.
- [46] S. Hu, Y. Wang, H. Li, The regulation effect of $\alpha 7$ nAChRs and M1AChRs on inflammation and immunity in sepsis, *Mediat. Inflamm.* 2021 (2021) 9059601, <https://doi.org/10.1155/2021/9059601>.
- [47] A.M. Kressel, T. Tsaava, Y.A. Levine, E.H. Chang, M.E. Addorisio, Q. Chang, B.J. Burbach, D. Carnevale, G. Lembo, A.M. Zador, U. Andersson, V.A. Pavlov, S. S. Chavan, K.J. Tracey, Identification of a brainstem locus that inhibits tumor necrosis factor, *Proc. Natl. Acad. Sci. U.S.A.* 117 (47) (2020) 29803–29810, <https://doi.org/10.1073/pnas.2008213117>.
- [48] B.B. Pinto, C. Ritter, M. Michels, et al., Characterization of brain-heart interactions in a rodent model of sepsis, *Mol. Neurobiol.* 54 (5) (2017) 3745–3752.
- [49] R. Sankowski, S. Mader, S.I. Valdés-Ferrer, Systemic inflammation and the brain: novel roles of genetic, molecular, and environmental cues as drivers of neurodegeneration, *Front. Cell. Neurosci.* 9 (2015) 28, <https://doi.org/10.3389/fncel.2015.00028>.
- [50] M.L. Xu, X.J. Yu, J.Q. Zhao, Y. Du, W.J. Xia, Q. Su, M.M. Du, Q. Yang, J. Qi, Y. Li, S.W. Zhou, G.Q. Zhu, H.B. Li, Y.M. Kang, Calcitriol ameliorated autonomic dysfunction and hypertension by down-regulating inflammation and oxidative stress in the paraventricular nucleus of SHR, *Toxicol. Appl. Pharmacol.* 394 (2020) 114950, <https://doi.org/10.1016/j.taap.2020.114950>.
- [51] M.H. Fu, I.C. Chen, C.H. Lee, C.W. Wu, Y.C. Lee, Y.C. Kung, C.Y. Hung, K. Wu, Anti-neuroinflammation ameliorates systemic inflammation-induced mitochondrial DNA impairment in the nucleus of the solitary tract and cardiovascular reflex dysfunction, *J. Neuroinflammation* 16 (1) (2019) 224, <https://doi.org/10.1186/s12974-019-1623-0>.

- [52] H.B. Li, Restorative effect of modified dioscorea pills on the structure of hippocampal neurovascular unit in an animal model of chronic cerebral hypoperfusion, *Heliyon* 5 (4) (2019) e01567, <https://doi.org/10.1016/j.heliyon.2019.e01567>.
- [53] D.L. Liu, Z. Hong, J.Y. Li, Y.X. Yang, C. Chen, J.R. Du, Phthalide derivative CD21 attenuates tissue plasminogen activator-induced hemorrhagic transformation in ischemic stroke by enhancing macrophage scavenger receptor 1-mediated DAMP (peroxiredoxin 1) clearance, *J. Neuroinflammation* 18 (1) (2021) 143, <https://doi.org/10.1186/s12974-021-02170-7>.
- [54] H.B. Li, X.J. Yu, J. Bai, Q. Su, M.L. Wang, C.J. Huo, W.J. Xia, Q.Y. Yi, K.L. Liu, L.Y. Fu, G.Q. Zhu, J. Qi, Y.M. Kang, Silencing salusin β ameliorates heart failure in aged spontaneously hypertensive rats by ROS-relative MAPK/NF- κ B pathways in the paraventricular nucleus, *Int. J. Cardiol.* 280 (2019) 142–151, <https://doi.org/10.1016/j.ijcard.2018.12.020>.
- [55] W.C. Weng, K.H. Lin, P.Y. Wu, Y.H. Ho, Y.L. Liu, B.J. Wang, C.C. Chen, Y.C. Lin, Y.F. Liao, W.T. Lee, W.M. Hsu, H. Lee, VEGF expression correlates with neuronal differentiation and predicts a favorable prognosis in patients with neuroblastoma, *Sci. Rep.* 7 (1) (2017) 11212, <https://doi.org/10.1038/s41598-017-11637-8>.
- [56] A. Abdullahi, S. Truijen, W. Saeys, Neurobiology of recovery of motor function after stroke: the central nervous system biomarker effects of constraint-induced movement therapy, *Neural Plast.* (2020) 9484298, <https://doi.org/10.1155/2020/9484298>.
- [57] W. Yang, L. Zhang, S. Chen, Q. Yao, H. Chen, J. Zhou, W. Chen, L. He, Y. Zhang, Longshengzhi capsules improve ischemic stroke outcomes and reperfusion injury via the promotion of anti-inflammatory and neuroprotective effects in MCAO/R rats, *Evid. base Compl. Alternative Med. : eCAM* 2020 (2020) 9654175, <https://doi.org/10.1155/2020/9654175>.
- [58] J. Oh, Y. Kim, D. Baek, Y. Ha, Malignant gliomas can be converted to non proliferating glial cells by treatment with a combination of small molecules, *Oncol. Rep.* 41 (1) (2019) 361–368, <https://doi.org/10.3892/or.2018.6824>.
- [59] N. Ghasemi, The evaluation of astaxanthin effects on differentiation of human adipose derived stem cells into oligodendrocyte precursor cells, *Avicenna J. Med. Biotechnol. (AJMB)* 10 (2) (2018) 69–74.
- [60] S.R. Challa, K.R. Nalamolu, C.A. Fornal, B.C. Wang, R.C. Martin, E.A. Olson, A.L. Ujjainwala, D.M. Pinson, J.D. Klopfenstein, K.K. Veeravalli, Therapeutic efficacy of matrix metalloproteinase-12 suppression on neurological recovery after ischemic stroke: optimal treatment timing and duration, *Front. Neurosci.* 16 (2022) 1012812, <https://doi.org/10.3389/fnins.2022.1012812>.
- [61] S. Kuhn, L. Gritti, D. Crooks, et al., Oligodendrocytes in development, myelin generation and beyond, *Cells* 8 (11) (2019) 1424.
- [62] D. Xie, F.C. Shen, S.R. He, et al., IL-1 β induces hypomyelination in the periventricular white matter through inhibition of oligodendrocyte progenitor cell maturation via FYN/MEK/ERK signaling pathway in septic neonatal rats, *Glia* 64 (4) (2016) 583–602.
- [63] Q. Han, Q. Lin, P. Huang, et al., Microglia-derived IL-1 β contributes to axon development disorders and synaptic deficit through p38-MAPK signal pathway in septic neonatal rats, *Neuroinflammation* 14 (1) (2017) 52.